Steel and Composite Structures, *Vol. 17, No. 5 (2014) 561-572*
DOI: http://dx.doi.org/10.12989/scs.2014.17.5.561

Scattering analysis of curved FSS using Floquet harmonics and asymptotic waveform evaluation technique

Yi-Ru Jeong [1a], Ic-Pyo Hong [2], Heoung-Jae Chun [3], Yong Bae Park [4], Youn-Jae Kim [5] and Jong-Gwan Yook [*1]

[1] *School of Electrical and Electronics Engineering, Yonsei University, Seoul, Korea*
[2] *Department of Information and Communication Engineering, Kongju National University, Cheonan, Korea*
[3] *School of Mechanical Engineering, Yonsei University, Seoul, Korea*
[4] *Department of Electrical and Computer Engineering, Ajou University, Suwon, Korea*
[5] *Agency for Defense and Development, Daejon, Korea*

(*Received March 20, 2013, Revised March 19, 2014, Accepted March 27, 2014*)

Abstract. In this paper, we present the scattering characteristics of infinite and finite array using method of moment (MoM) with Floquet harmonics and asymptotic waveform evaluation (AWE) technique. First, infinite cylindrical dipole array is analyzed using the MoM with entire domain basis function and cylindrical Floquet harmonics. To provide the validity of results, we fabricated the cylindrical dipole array and measured the transmission characteristics. The results show good agreements. Second, we analyzed the scattering characteristics of finite array. A large simulation time is needed to obtain the scattering characteristics of finite array over wide frequency range because Floquet harmonics can't be applied. So, we used the MoM with AWE technique using Taylor series and Pade approximation to overcome the shortcomings of conventional MoM. We calculated the radar cross section (RCS) as scattering characteristics using the proposed method in this paper and the conventional MoM for finite planar slot array, finite spherical slot array, and finite cylindrical dipole array, respectively. The compared results agree well and show that the proposed method in this paper is good for electromagnetic analysis of finite FSS.

Keywords: frequency selective surface; finite and curved array; cylindrical Floquet harmonics; asymptotic waveform evaluation (AWE) technique; RCS; transmission

1. Introduction

Frequency selective surfaces (FSS) have been used for obtaining band-stop or band-pass characteristics over a wide range of the electromagnetic spectrum. These properties can be gained from periodic array structure. FSS has various applications such as reflector antenna which can operate at two different frequencies and FSS radome which can provide transparent characteristics at only the antenna's operating frequency. When FSS was combined with composite materialsor active device, EM characteristics were presented (Kim *et al*. 2006, Tennant and Chambers 2004). Recently, application of FSS for secure building from electromagnetic signal gets attention and

*Corresponding author, Professor, E-mail: jgyook@yonsei.ac.kr
[a] Ph.D. Student, E-mail: yiruta@naver.com

Copyright © 2014 Techno-Press, Ltd.
http://www.techno-press.org/?journal=scs&subpage=8 ISSN: 1229-9367 (Print), 1598-6233 (Online)

reinforced concrete structure which has periodically arranged steel bars is becoming the issues for the electromagnetic shielding as well as mechanical property (Hyun *et al*. 2012, Choi *et al*. 2012).

The electromagnetic analysis of FSS has been much investigated. Mainly, these researches are restricted to infinite planar array (Lee *et al*. 2011, Lee *et al*. 2013). Analysis about finite and curved FSS is required because FSS may be applied to finite and curved structure like radome on the aircraft. But, researches about finite and curved FSS are insufficient. Besides, there is no validation of the calculation result in many papers through the experiment to prove the accuracy of algorithms. Therefore it is required to examine the accuracy of algorithms for the analysis of curved FSS through the experiment and compare the calculation result of various algorithms.

In previous papers, cylindrical Floquet harmonics are applied to analyze the scattering characteristics of cylindrical FSS because cylindrical infinite array has the strict periodicity mathematically. Basically, cylindrical Floquet harmonics for analysis of strip array were studied (Cwik 1990, Uzer and Ege 2004). After that time, strip array in multilayer and slot array were researched. In these papers, there is no validation of calculation result through experiment. So, comparison between calculation and experiment is required (Jeong *et al*. 2012).

In case of the curved FSS with arbitrary curvature, general numerical technique like MoM for arbitrary shaped perfect electric conductor (PEC) bodies should be used due to imperfect periodicities mathematically. MoM in frequency domain is suitable to scattering analysis of PEC (Gibson 2007). But, a great deal of calculation time for wide-band analysis is required because the calculation for inverse of matrix should be repeated in every frequency. The AWE technique is used to achieve fast frequency sweeping (Cockrell and Beck 1996). Electric surface currents at an arbitrary frequency are calculated by polynomial expansion. So, surface current for wide-band analysis can be predicted. The AWE is combined with MoM in frequency domain (Reddy *et al*. 1998, Ma *et al*. 2012). Furthermore, the research for available bandwidth estimation of AWE is progressed (Peng and Sheng 2008).

In this paper, scattering characteristics such as RCS and transmission of cylindrical infinite dipole array is first analyzed using MoM with entire domain basis function and cylindrical Floquet harmonics. In order to verify the calculation result, the cylindrical dipole array is fabricated and the experiment about transmission characteristics is conducted. Second, RCS of finite cylindrical dipole array is calculated using the MoM with AWE. Conventional MoM for arbitrary shape PEC needs the large calculation time. But, if AWE using Talyor series and Pade approximation is applied to MoM, calculation time for wide-band analysis is reduced drastically. Finally, RCS of finite planar slot array, finite spherical slot array, and finite cylindrical dipole array is obtained with conventional MoM and MoM with AWE technique, respectiviely.

2. Infinite cylindrical array

l and the width is w are infinitely arranged along z direction. Also, N patches are placed along the circumference of the circle. The periodicities of the structure for the z direction and ϕ directions are T_z and $T_\phi = 2\pi/N$. The cylindrical surface where dipole patches are placed is located at $\rho = \rho_0$. Then, arbitrarily polarized wave is incident from a direction (θ^{inc}, ϕ^{inc}).

2.1 Cylindrical Floquet harmoncis

Periodic structures can be analyzed with Floquet harmonics efficiently. If periodic structure is

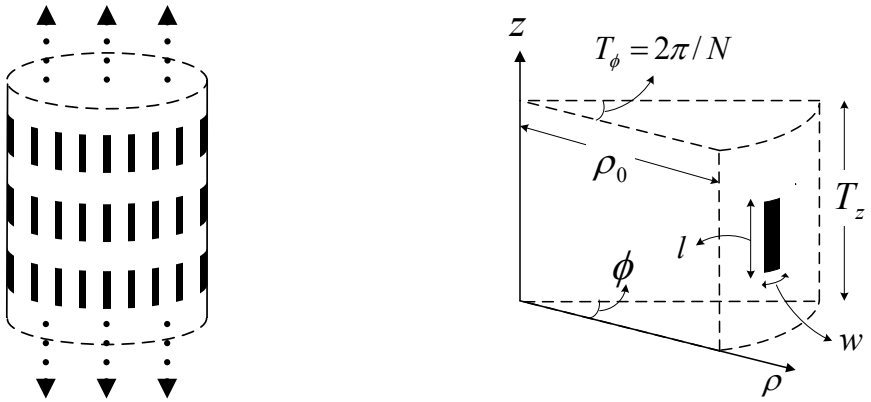

Fig. 1 (a) Structure of a cylindrical infinite array; (b) Unit cell

excited by a cylindrical wave, scattered waves should be represented as infinite sums of periodic function. These periodic functions are called the Floquet harmonics. Scattered waves can be expressed using the Floquet harmonics because they are periodic solutions of differential equations and a complete orthogonal set of periodic functions. The Floquet harmonics for planar periodic array can be obtained in Cartesian coordinate system and are well known. To analyze the cylindrical periodic array, the Floquet harmonics should be found in cylindrical coordinate system.

Basically, the cylindrical Floquet harmonics are the solutions of a scalar Helmhotz wave equation in a source free region.

$$\left(\nabla^2 + k^2\right) A_p(\rho, \phi, z) = 0 \tag{1}$$

where A_p is a vector potential and p tells its polarization such as TM (transverse magnetic) or TE (transverse electric). k is the wave number and f is the frequency. Besides, the solutions should satisfy the periodicity requirements for z direction and ϕ directions as follows

$$A_p(\rho, \phi, z + T_z) = A_p(\rho, \phi, z) e^{-j\beta_0 T_z} \tag{2a}$$

$$A_p(\rho, \phi + T_\phi, z) = A_p(\rho, \phi, z) e^{-jv_0 T_\phi} \tag{2b}$$

$$A_p(\rho, \phi + 2\pi, z) = A_p(\rho, \phi, z) \tag{2c}$$

where v_0 is an integer and $\beta_0 = k \cos^{inc}$ is the phase constant of the incident wave for the z direction. Eqs. (2)-(3) are determined by the geometry of unit cell and Eq. (4) is fundamental condition for the cylinder structure. Cylindrical Floquet harmonics which satisfy periodic boundary conditions for the z and ϕ variables (Cwik 1990) is given by

$$\psi_{mn}(\phi, z) = \frac{1}{(T_\phi T_z)^{1/2}} e^{-jv_m \phi} e^{-j\beta_n z} \tag{3a}$$

$$\beta_n = \beta_0 + 2\pi\, n/T_z, \quad v_m = v_0 + 2\pi\, m/T_\varphi \tag{3b}$$

Cylindrical Floquet harmonics for the ρ variable are Bessel functions or Hankel functions because there is no need to consider the periodic boundary conditions in the ρ direction. Written completely, the vector potential can be expressed as the infinite sum of the Floquet harmonics as follows

$$A_p(\rho,\phi,z) = \begin{cases} \sum_{m=-\infty}^{\infty}\sum_{n=-\infty}^{\infty} a_{p,mn}\psi_{mn}(\phi,z)J_{v_m}(\kappa_n\rho), & \rho < \rho_0 \\ \sum_{m=-\infty}^{\infty}\sum_{n=-\infty}^{\infty} a_{p,mn}\psi_{mn}(\phi,z)H^{(2)}_{v_m}(\kappa_n\rho), & \rho > \rho_0 \end{cases} \tag{4}$$

where $a_{p,mn}$ is the unknown coefficient and κ_n is $\sqrt{k^2-\beta_n^2}$. Vector potentials are calculated from truncated sum because it impossible to use the infinite sum really.

2.2 RCS and transmission

First, the scattered fields can be obtained from vector potentials which are expressed as the infinite sum of the Floquet harmonics. Then, if the boundary conditions which force the electric field to be continuous and the magnetic field to be discontinuous are applied to inner field and outer field of FSS, the scattered fields can be represented in terms of the induced surface current on the dipole patches. The unknown coefficients of vector potentials for outside of FSS is expressed with the surface current which is expanded into entire domain basis function as follows

$$J_z = \sum_{q=1}^{Q} c_q \sin\left\{\frac{q\pi}{l}\left(z+\frac{l}{2}\right)\right\} \tag{5}$$

where J_z is the surface current for the z direction and q is the number of used basis function. The surface current J_ϕ for the ϕ direction is ignored because it is assumed that width of strips is very narrow. An electric field integral equation is obtained by equating total tangential electric fields to zero across the patch. This integral equation expresses surface current in respect of incident fields. Then, if Galerkin's method is applied to an electric field integral equation, matrix form can be obtained (Gibson 2007). This resulting matrix size is small because entire domain functions are used. Finally, once this matrix equation is solved, the surface current distribution can be obtained.

When an incident wave is a plane wave ($\mathbf{E}^{inc}$) in a direction, the RCS can be calculated. A plane wave should be decomposed into the cylindrical waves and the scattered field ($\mathbf{E}^{s}$) for each cylindrical wave is obtained because the cylindrical Floquet harmonics are developed in the cylindrical coordinates. Final scattered field is the sum of each scattered fields. RCS is calculated using scattered field in far-region as follows

$$\mathrm{RCS} = \lim_{\rho\to\infty} \frac{\left|E^s\right|^2}{\left|E^{inc}\right|^2} \tag{6}$$

where the magnitude of the scattered field is normalized to that of the plane wave. When the transmission characteristics are obtained, incident wave is the cylindrical wave which is radiated

from infinite line current source in the origin. This cylindrical wave is expressed with Hankel functions. Scattered field across FSS is evaluated at infinity. Then total field is sum of scattered fields from cylindrical FSS and incident fields in the absence of cylindrical FSS. The magnitude of the total field is normalized to that of the incident wave that would exist at the infinity if the cylindrical FSS were not present.

$$\text{Transmission} = \lim_{\rho\to\infty} \frac{\left|\mathbf{E}^{inc} + \mathbf{E}^{s}\right|^2}{\left|\mathbf{E}^{inc}\right|^2} \tag{7}$$

2.3 Results with cylindrical Floquet harmonics

32 (N = 32) dipole patches with w of 4 mm and l of 6 cm are arranged along circumference of cylinder. The periodicities T_z for the z direction is 100 mm and the radius ρ_0 of the cylinder is 250 mm. When the TM polarized plane wave is incident from a direction (θ^{inc} = 90°, ϕ^{inc} = 0°), RCS of cylindrical infinite array is shown in Fig. 2. The scattered fields are observed in the back side (ϕ^s = 180°) of the structure and in the front side (ϕ^s = 0°) of the structure. In general, RCS at ϕ^s = 180° is greater than RCS at ϕ^s = 0°. RCS for variation of frequency is gradual at ϕ_s = 180°. But, RCS for variation of frequency is irregular at ϕ_s = 0° and RCS changes much.

In Fig. 3(b), the calculation result and experiment result of transmission characteristics are compared. When incident wave is the cylindrical wave from infinite electric line source at the origin, the transmission characteristics are obtained. To validate calculation results, we fabricated the cylindrical dipole array. The experiment for transmission characteristics is performed as shown Fig. 3(a). Two antennas are located on both sides of FSS and materials which absorb the electromagnetic signal are placed around FSS. In order to obtain the transmission characteristics, the difference of measured value in network analyzer between the case in the presence of FSS and the case in the absence of FSS is obtained. And moving averages are applied to the measured data to remove ripples due to multiple reflections between the two antennas (Joumayly *et al*. 2009). Both calculation and experiment have the band-stop characteristics and the resonant frequency is around 2.5 GHz. Experiment result agrees well with the calculation result.

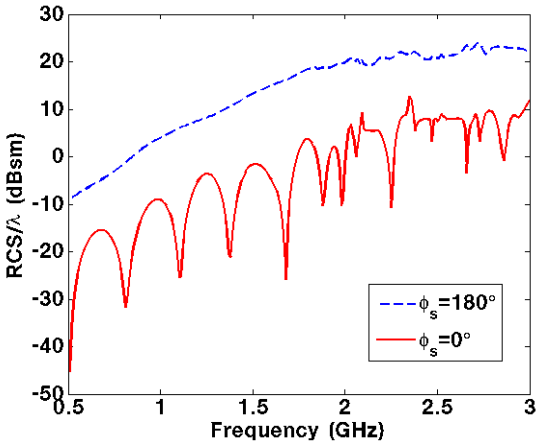

Fig. 2 RCS at ϕ^s = 0° and ϕ^s = 0°

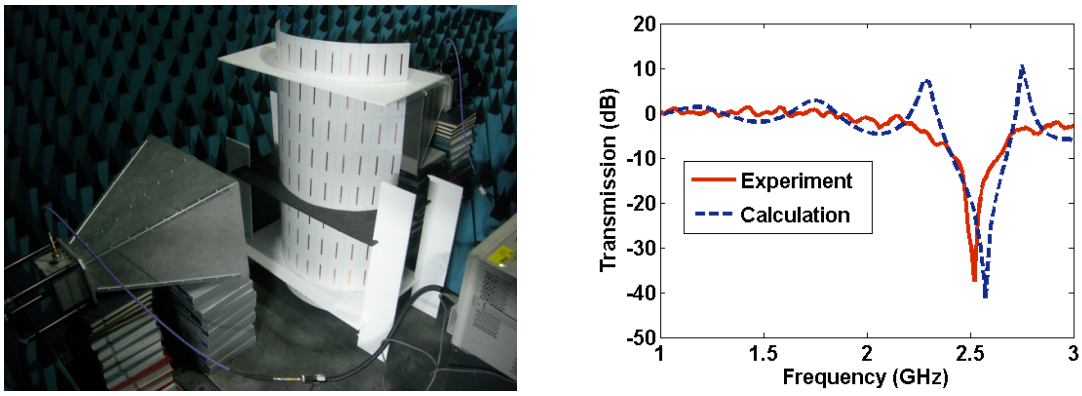

(a) (b)

Fig. 3 (a) Experiment for transmission of FSS; (b) Transmission comparison between experiment and calculation

3. Finite and curved array

3.1 MoM in the frequency domain

When plane wave is incident from a direction (θ^{inc}, ϕ^{inc}), the total tangential electric field should be zero. Electric field integral equation can be induced because the sum of scattered field and incident field should be zero as follows

$$\mathbf{E}^{scat} + \mathbf{E}^{inc} = 0 \tag{8}$$

To analyze an arbitrary PEC body, PEC surface is divided into subdomain and RWG function is used as basis function of surface current. Galerkin's method is that electric field integral equations are multiplied by vector testing functions and integrated over the surface of PEC body. If this method is applied to electric field integral equations, matrix equation can be obtained (Gibson 2007) as follows

$$Z(k_0)I(k_0) = V(k) \tag{9a}$$

$$Z(k) = \frac{jk\eta_0}{4\pi}\iint \mathbf{T}\cdot\iint \mathbf{J}\frac{e^{-jkR}}{R}ds'ds - \frac{j\eta_0}{4\pi k}\iint(\nabla\cdot\mathbf{T})\iint(\nabla'\cdot\mathbf{J})\frac{e^{-jkR}}{R}ds'ds \tag{9b}$$

$$V(k) = \iint \mathbf{T}\cdot\mathbf{E}^{inc}ds \tag{9c}$$

where $Z(k)$ is the complex and dense impedance matrix and $V(k)$ is the excitation vector. $I(k)$ is the unknown current coefficient vector. **J** is basis function and **T** is testing function. When this matrix equation is solved at any frequency, surface current distribution on the PEC body is known. At this time, as matrix size becomes larger, calculation time is longer exponentially. Finally, the scattered field can be calculated from the surface current.

3.2 AWE technique

3.2.1 Taylor series

The surface currents arefound from calculation result of Eq. (9a) at any frequency. But, calculation time is very longer over wide-band frequencies because inverse operation of matrix should be repeated in every frequency. Therefore it is efficient to use the AWE technique for wide-band analysis. The AWE technique is that the unknown currents coefficient at any frequency f are expanded in Taylor series and the moments of Taylor series are obtained from impedance matrix and excitation vector at particular frequency, f_0. Equations about Taylor series $I(k)$ and the moments m_n are given (Cockrell *et al*.1996) by

$$I(k) = \sum_{n=0}^{\infty} m_n (k - k_0)^n \tag{10a}$$

$$m_n = Z^{-1}(k_0)\left[\frac{V^{(n)}(k_0)}{n!} - \sum_{q=1}^{n} \frac{Z^{(q)}(k_0) m_{n-q}}{q!}\right] \tag{10b}$$

where $Z^{(q)}(k_0)$ is the qth derivative with respect to k of $Z(k_0)$ and $V^{(n)}(k_0)$ is the nth derivative with respect to k of $V(k_0)$. Using the calculated moments previously, the surface currents at different frequencies can be obtained very quickly from Taylor series.

3.2.2 Pade approximation

When frequency is beyond the radius of convergence, Talyor series is divergent. Generally, there is a limit to the accuracy of Tayloer series due to the short radius of convergence. In order to overcome this drawback, Pade approximation which uses a rational function is applied. Taylor series can be often improved by being rearranged into a ratio of two such expansions. Pade approximation is given (Reddy *et al*. 1998) by

$$I_{pade}(k) = \frac{P_L(k)}{Q_M(k)} = \frac{\sum_{i=0}^{L} a_i (k - k_0)^i}{1 + \sum_{i=1}^{M} b_i (k - k_0)^i} \tag{11}$$

From a truncated Taylor expansion, the corresponding Pade coefficients are determined by requiring that the Taylor expansion is matched with a rational function lik Eq. (12).

$$\sum_{n=0}^{L+M} m_n (k - k_0)^n = \frac{P_L(k - k_0)}{Q_M(k - k_0)} \tag{12}$$

After multiplying up the denominator and then equating coefficients up to x^{L+M}, the resulting simultaneous equations whose size is $L + M + 1$ are obtained. Then the unknown coefficients of Pade approximation are found.

3.3 Bandwidth estimation of AWE

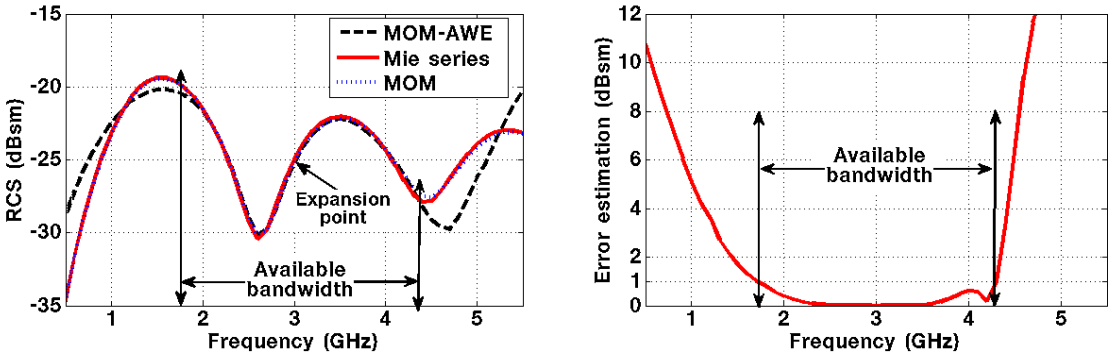

(a) (b)

Fig. 4 (a) RCS of a conducting sphere with MoM with AWE, analytic solution; and MoM (b) Estimated error of AWE

Until now, the AWE technique in a particular expansion point k_0 has been searched. In addition, it is important to determine the available bandwidth for a desired accuracy because the bandwidth of satisfying a desired accuracy is limited in one expansion point. To estimate the available bandwidth, the error of AWE about true solution should be calculated. First, the exact error of the AWE technique is given (Peng *et al*. 2008) by

$$E_n = \left|I(x) - I_{pade}(x)\right| = \left|\sum_{k=0}^{\infty} m_k x^k - \frac{P_n(x)}{Q_n(x)}\right| = \frac{x^{2n+1}}{Q_n(x)} \sum_{k=0}^{\infty} r_k x^k \tag{13a}$$

$$r_k = \sum_{i=0}^{n} b_i m_{2n+k+1-i} \tag{13b}$$

where r_k is determined by matching the coefficients on both sides.

To obtain the true error of the AWE technique, infinite sum in Eq. (13a) should be calculated. But the estimated error can only be found because the known moments of Taylor series are finite. At $L = M = n$, only r_0 can be calculated. It is assumed that the higher terms such as r_1, r_2, r_3, etc. are ignorable. Finally, the error estimation is given by

$$E_n = \left|I(x) - I_{pade}(x)\right| \cong \frac{x^{2n+1}}{Q_n(x)} |r_0| \tag{14a}$$

$$r_0 = \sum_{i=0}^{n} b_i m_{2n+1-i} \tag{14b}$$

As shown in Fig. 4(a), the monostatic RCS of a conducting sphere with a radius of 3.1 cm is computed. Also, the estimated error of AWE is shown in Fig. 4(b). One expansion point is located at 3 GHz and 8 order ($L = 4$, $M = 4$) rational function is used. It can be inferred that the result using MoM is reliable because the result with MoM is very similar to analytic solution (Mie series). When it is hoped that the difference between true result and result with the AWE is lower

than 1 dB, it is known that available frequency range is from 1.8 GHz to 4.2 GHz as shown in Fig. 4(b). Available frequency range from Fig. 4(b) is similar to it from Fig. 4(a). This result shows that even though true solutions are unknown, the error estimation technique can be used to determine the available bandwidth of the AWE technique. If desired bandwidth is from 0.5 GHz to 5 GHz for this sphere structure, AWE at one expansion point is not enough. Therefore AWE at several expansion points should be applied.

If available bandwidth from one expansion point is shorter than desired bandwidth, the AWE technique should be applied at a multiple of expansion point. First, the lowest frequency f_L and the highest frequency f_H are set. Second, the AWE technique is applied at a mid-point frequency $f = 0.5(f_L + f_H)$. Then the available bandwidth is obtained using the error estimation technique about AWE. If the available bandwidth doesn't satisfy the desired bandwidth, AWE technique is applied at mid-point frequencies of the remaining bandwidth again. This process is repeated until the surface current distribution is found over the desired bandwidth.

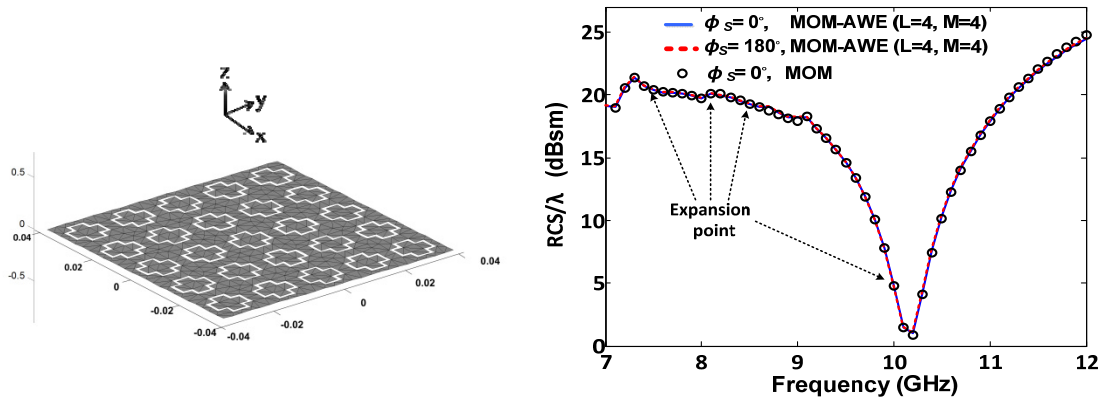

(a) (b)

Fig. 5 Finite planar slot array (a) structure; (b) RCS

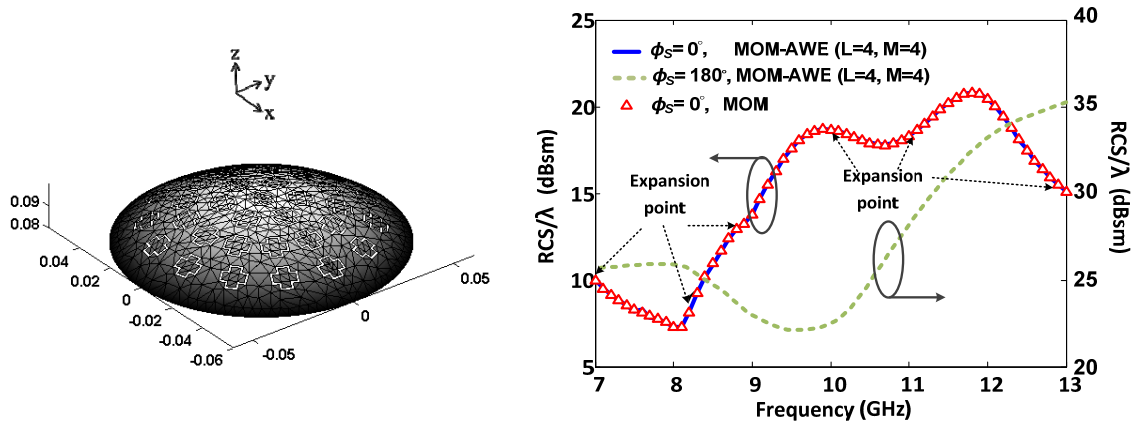

(a) (b)

Fig. 6 Finite spherical slot array (a) structure; (b) RCS

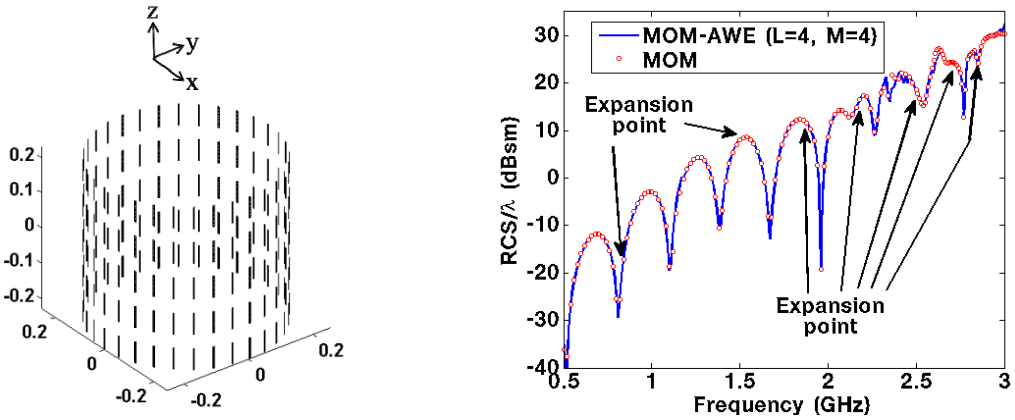

(a) (b)

Fig. 7 Finite cylindrical dipole array (a) structure; (b) Monostatic RCS

3.4 Results with AWE technique

When incident wave is plane wave, RCS of finite and curved FSS is calculated with the AWE technique. The AWE technique is applied at a multiple of expansion point over large bandwidth. When plane wave is incident from a direction (), RCS of finite planar slot array which is located on x-y plane is shown in Fig. 5(b). Overall size of structure as shown Fig. 5(a) is 8 cm × 8 cm and the number of arranged slots is 25. RCSs for $\theta^s = 0°$ and $\theta^s = 180°$ are same as shown Fig. 5(b) because bistatic RCS pattern for θ direction is symmetrical. The resonant frequency is around 10 GHz. At the resonant frequency, total field is similar to incident field because scattered field is very small. This is interpreted as frequency selective transmission of signals. In Fig. 6(a), slots are arranged on the spherical surface. Overall size is about 12 cm × 12 cm × 10 cm and the number of arranged slots is 34. When plane wave is incident from a direction ($\theta^{inc} = 0°$), RCS of finite spherical slot array which is located on the curved surface is shown in Fig. 6(b). Compared to Fig. 5(b), the resonant frequency of finite spherical slot array is changed. Absolute value of RCS for $\theta^s = 0°$ is different with it for $\theta^s = 180°$ and changing trend of RCS for $\theta^s = 0°$ is contrary to it for $\theta^s = 0°$. It can be inferred that finite spherical array also has selective transmission of electromagnetic wave according to frequency.

When plane wave is incident from a direction ($\theta^{inc} = 90°$), monostatic RCS of finite cylindrical dipole array is shown in Fig. 7(b). As shown Fig. 7(a), 32 ($N = 32$) dipole patches with w of 4 mm and l of 6 cm are arranged along circumference of cylinder. The 5 dipoles are placed along the z direction with 100 mm of spacing and the radius ρ_0 of the cylinder is 250 mm. RCS pattern versus frequency in Fig. 7(b) is more complex than it in Figs. 5(b) and 6(b). These result shows scattering characteristics of finite and curved array. Also, it is possible to calculate RCS efficiently with MoM using AWE technique.

4. Conclusions

Using MoM with cylindrical Floquet harmonics, both RCS and transmission characteristics of

cylindrical infinite dipole array can be found efficiently. Thanks to mathematical periodicity, cylindrical Floquet harmonics can be used. To verify the calculation result, the cylindrical dipole array is fabricated and the transmission characteristics are measured. Experiment result is similar to the numerical result. So, it can be inferred that cylindrical Floquet harmonics is suitable for the scattering analysis of cylindrical infinite array.

MoM with subdomain basis function should be used to analyze curved and finite FSS with arbitrary curvature. Also, the AWE using Taylor series and Pade approximation is applied to the scattering analysis of finite array for effective calculation. When plane wave is incident, RCS of finite planar slot array, finite spherical slot array, and finite cylindrical dipole array is obtained, respectively. Calculation results between conventional MoM and MoM using AWE technique are similar and show that MoM using AWE is good for electromagnetic analysis of finite FSS.

Acknowledgments

This work has been supported by the Low Observable Technology Research Center Program of the Defense Acquisition Program Administration and the Agency for Defense Development of Republic of Korea.

References

Choi, E.G., Kim, H.S. and Shin, Y.S. (2012), "Performance of fire damaged steel reinforced high strength concrete (SRHSC) columns", *Steel Compos*. *Struct*., *Int*. *J*., **13**(6), 521-537.

Cockrell, C.T. and Beck, F.B. (1996), "Asymptotic waveform evaluation (AWE) technique for frequency domain electromagnetic analysis", NASA Tech. Memo 110292.

Cwik, T. (1990), "Coupling into and scattering from cylindrical structures covered periodically with metallic patches", *IEEE Trans*. *Antennas Propagat*., **38**(2), 220-226.

Gibson, W.C. (2007), *The Method of Moments in Electromagnetics*, CRC press, USA.

Hyun, S.Y., Lee, K.W. and Yook, J.G. (2012), "Modeling of shielding effectiveness of reinforced concrete walls for electromagnetic pulse", *Proceedings of the 9th European Radar Conference*, Amsterdam, Netherland, October.

Jeong, Y.R., Lee, K.W., Hong, I.P., Chun, H.J., Lee, M.G. and Yook, J.G. (2012), "Scattering of cylindrical FSS with rectangular patch array", *Antennas and Propagation Society International Symposium* (*APSURSI*), Chicago, IL, USA, July.

Joumayly, M.A. and Behdad, N. (2009), "A new technique for design of low-profile second-order bandpass frequency selective surfaces", *IEEE Trans*. *Antennas Propagt*., **57**(2), 452-459

Kim, P.C., Chin, W.S., Lee, D.G. and Seo, I.S. (2006), "EM characteristics of the RAS composed of E-glass/epoxy composite and single dipole FSS element", *Compos*. *Struct*., **75**(1-4), 601-609.

Lee, H.M. and Kim, Y.J. (2010), "Double-layered frequency selective surface superstrate using ring slot and dipole-shaped unit cell structure", *J*. *Electromagnet*. *Eng*. *Sci*., **10**(3), 86-91.

Lee, K.W., Jeong, Y.R., Hong, I.P., Lee, M.G., Chun, H.J. and Yook, J.G. (2011), "Simple design method of FSS radome analysis using equivalent circuit model", *IEICE Electron*. *Express*, **8**(23), 2002-2009.

Lee, S., Rhee, S.Y., Kim, P.Y. and Kim, N. (2013), "Realization of high impedance surface characteristics using a periodically transformed artificial magnetic conductor structure and reduction technique of specific absorption rate", *J*. *Electromagnet*. *Eng*. *Sci*., **13**(2), 113-119.

Ma, J., Gong, S.X., Wang, X., Liu, Y. and Xu, Y.X. (2012), "Efficient wide-band analysis of antennas around a conducting platform using MOM-PO hybrid method and asymptotic waveform evaluation technique", *IEEE Trans*. *Antennas Propagat*., **60**(12), 6048-6052.

Peng, Z. and Sheng, X.Q. (2008), "A bandwidth estimation approach for the asymptotic waveform evaluation technique", *IEEE Trans*. *Antennas Propagat*., **56**(3), 913-917.
Reddy, C.J., Deshpande, M.D., Cockrell, C.T. and Beck, F.B. (1998), "Fast RCS computation over a frequency band using method of moments in conjunction with asymptotic waveform evaluation technique", *IEEE Trans*. *Antennas Propagat*., **46**(8), 1229-1223.
Tennant, A. and Chambers, B. (2004), "Adaptive radar absorbing structure with PIN diode controlled active frequency selective surface", *Smart Mater*. *Struct*., **13**(1), 122-125.
Uzer, A. and Ege, T. (2004), "Radiation from a current filament located inside a cylindrical frequency selective surface", *ETRI J*., **26**(5), 481-485.

CC

This work was presented in CODE 2012 on November 13-16, 2012, Jeju, Korea.
(The 2nd International Conference in Computational Design in Engineering)